

Palladium(0) Nanoparticles on Glass-Polymer Composite Materials as Recyclable Catalysts: A Comparison Study on their Use in Batch and Continuous Flow Processes

Klaas Mennecke,^a Raul Cecilia,^b Toma N. Glasnov,^c Susanne Gruhl,^d Carla Vogt,^d Armin Feldhoff,^e M. A. Larrubia Vargas,^f C. Oliver Kappe,^{c,*} Ulrich Kunz,^{b,*} and Andreas Kirschning^{a,*}

^a Center of Biomolecular Drug Research (BMWZ) and Institute of Organic Chemistry, Leibniz Universität Hannover, Schneiderberg 1B, 30167 Hannover, Germany

Fax: (+49)-511-762-3011; e-mail: andreas.kirschning@oci.uni-hannover.de

^b Institute of Chemical Process Engineering (ICVT), Clausthal University of Technology, Leibnizstr. 17, 38678 Clausthal-Zellerfeld, Germany

E-mail: kunz@icvt.tu-clausthal.de

^c Christian Doppler Laboratory for Microwave Chemistry and Institute of Chemistry, Karl Franzens University, Heinrichstraße 28, 8010 Graz, Austria

E-mail: oliver.kappe@uni-graz.at

^d Institute of Inorganic Chemistry, Leibniz Universität Hannover, Callinstraße 9, 30167 Hannover, Germany

^e Institute of Physical Chemistry and Electrochemistry, Leibniz Universität Hannover, Callinstraße 3-3A, 30167 Hannover, Germany

^f Chemical Engineering Department, University of Malaga, Campus de Teatinos, 29071 Malaga, Spain

Received: October 23, 2007; Published online: March 17, 2008



Supporting information for this article is available on the WWW under <http://asc.wiley-vch.de/home/>.

Abstract: Palladium particles were generated by reduction of palladate anions bound to an ion exchange resin inside microreactors. The size and distribution of the palladium particles differed substantially depending on the degree of cross-linking and the density of ion exchange sites on the polymer/glass composites, the latter parameter having a larger influence than the former. The polymer phase of the composite materials was used for the loading with clusters composed of palladium particles which are 1 to 10 nm in diameter. The reactivity and stability of six different palladium-doped polymer/glass composite samples for transfer hydrogenations was investigated both under conventional and microwave heating in the batch mode as well as under continuous

flow conditions using the cyclohexene-promoted transfer hydrogenation of ethyl cinnamate as a model reaction. Regarding the heating method it was found that catalysts that are composed of larger metal particles perform better under microwave irradiating conditions whereas samples with smaller particle sizes perform better under conventional heating. Comparing batch experiments with flow-through experiments the latter technique gives better conversion. Reusability was better in microwave heated experiments than in traditional heating.

Keywords: enabling technologies; hydrogenation; immobilization; microreactors; microwave heating; palladium

Introduction

The role of metal nanoparticles, particularly Pd(0) clusters as active catalytic species has increased dramatically in recent years. This field, sometimes termed “semi-heterogeneous catalysis”, is located at the frontier between homogeneous and heterogeneous catalysis.^[1] Nanoparticles often offer higher catalytic efficiency per gram than larger size materials, be-

cause of their large surface-to-volume ratio. Usually, catalytically active nanoparticles are prepared from a metal salt, a reducing agent, and a stabilizer and are supported on an oxide,^[2] charcoal,^[3] a zeolite^[4] or a polymer.^[5] Physical methods for preparation, such as the electrochemical route developed by Reetz,^[6] are also numerous.^[7,8] Currently, several diverse protocols for preparing nanoparticles are being pursued such as impregnation,^[9] co-precipitation,^[9,10] deposition/pre-

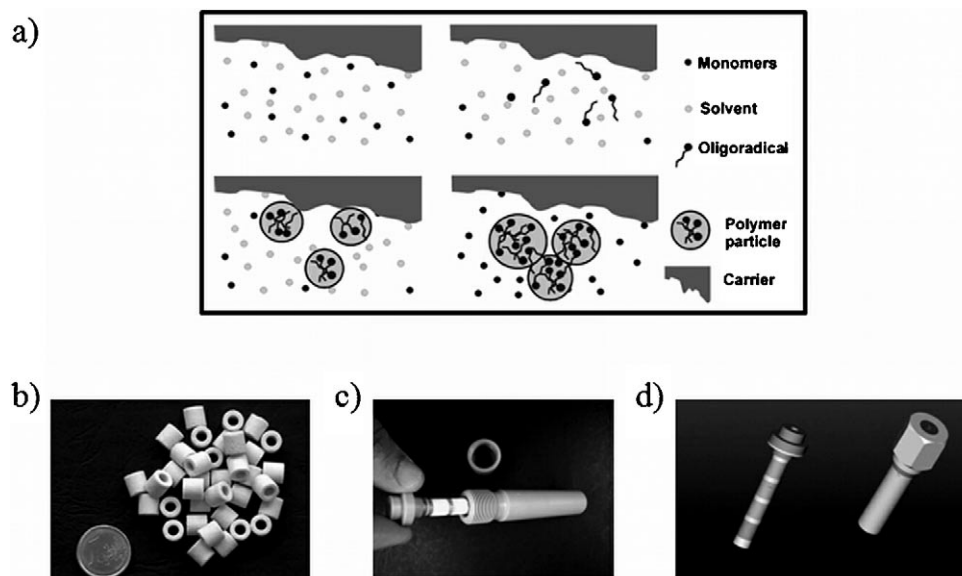


Figure 1. PASSflow reactor system as employed in the present work: a) Precipitation polymerization inside a megaporous glass carrier; b) monolithic porous glass polymer composite Raschig rings inserted into a c) PASSflow reactor (rings are aligned on a perforated tube; gaskets between the rings prevent bypass); d) housing is made of PEEK polymer. The flow streams from an annular gap through the ring walls and irregular microchannels inside the glass/polymer composite and leaves through the perforated inner tube (9 mm ring diameter).

precipitation,^[11] sol-gel,^[9,12] gas-phase organometallic deposition,^[13] sonochemical,^[14] micro-emulsion,^[15] laser ablation,^[16] electrochemical,^[17] and cross-linking modalities.^[18]

Polymers provide stabilization for Pd(0) nanoparticles through the framework or by binding weakly to the nanoparticle surface through a heteroatom that plays the role of a ligand. In this context, poly(*N*-vinyl-2-pyrrolidone) has been employed for nanoparticle stabilization and catalysis most frequently.^[18,19] Other polymers have recently been used as efficient supports for nanoparticle catalysis such as polyurea,^[20] polyacrylonitrile and/or polyacrylic acid,^[21] polysilane micelles with cross-linked shells,^[22] polysiloxanes,^[23] poly(4-vinylpyridine),^[24] poly(*N,N*-dialkylcarbodiimide),^[25] polyethylene glycol,^[26] chitosan^[27] and hyperbranched aromatic polyamides.^[28]

By taking advantage of ionic stabilization of palladium(0) particles^[29] we demonstrated that these particles can be generated after reduction of palladate anions loaded on anion exchange resins [obtained by precipitation polymerization inside the void volume of megaporous glass^[30] using chloromethylvinylbenzene (VBC) and divinylbenzene (DVB) as cross-linker].^[31] Beneficially, the deposition of palladium was carried out on the surface of this monolithic glass/polymer composite material inside a PASSflow reactor, a continuous flow system which was developed in our laboratories (Figure 1). This reactor concept has the unique feature that it can be operated at a wide range

of volumetric flow rates thereby reducing mass transfer phenomena.^[32–34]

The catalytic flow system showed excellent properties in transfer hydrogenations of alkenes, alkynes, benzyl ethers and aromatic nitro compounds. Additionally, we demonstrated that the Pd species performs C–C cross coupling reactions such as the Suzuki–Miyaura, the Heck, and the Sonogashira reactions under continuous flow conditions.^[31] This preliminary work had focussed on the scope of applicability of Pd(0) species inside these continuous flow reactors. At that point we speculated that the procedure had generated Pd(0) nanoparticles because of the high reactivity of the catalytic system and its long lifetime. In view of the importance of ligand-free, Pd-catalyzed transformations in the industrial context, it is of fundamental importance to relate the nature of the polymeric support, its composition, its swelling properties and its texture with the performance, stability and reusability of metal nanoparticles in catalytic transformations for which hardly any information has been accumulated so far.^[24b,35] In addition, it is unknown how the mode of heating (thermal heating or microwave irradiation) as well as the type of process (batch or continuous flow) chosen, effects nanoparticle-mediated catalysis. For investigating the influence of microwave irradiation^[36] on nanoparticle structure and the catalytic process in general, the PASSflow reactor shown in Figure 1c was fitted into a commercially available single mode microwave reactor de-

signed for continuous flow processing.^[37] Several recent publications have demonstrated the feasibility and benefits of carrying out metal-mediated flow chemistry under microwave conditions, although the influence of microwave irradiation on the heterogeneous metal catalyst itself has not been studied in detail.^[38] One of the advantages of microwave dielectric heating over conventional heating in the work described here is the fact that strongly absorbing materials such as metal particles can be heated selectively in a reaction mixture.^[36,39] It can therefore be imagined that the intrinsic temperature localized around those particles is significantly higher than that of the bulk solution.^[36,39] In the development of our reactor concept (Figure 1) we incorporated the opportunity to selectively heat (“activate”) the palladium nanoparticles by microwave irradiation since both the chosen reactor material (PEEK) as well as the porous glass polymer composite Raschig rings can be considered to be microwave transparent (see below).^[40] Our detailed studies in this field are disclosed in this account which focuses on the catalytic performance of Pd nanoparticles under different conditions and experimental set-ups.

Results and Discussion

Ion Exchange

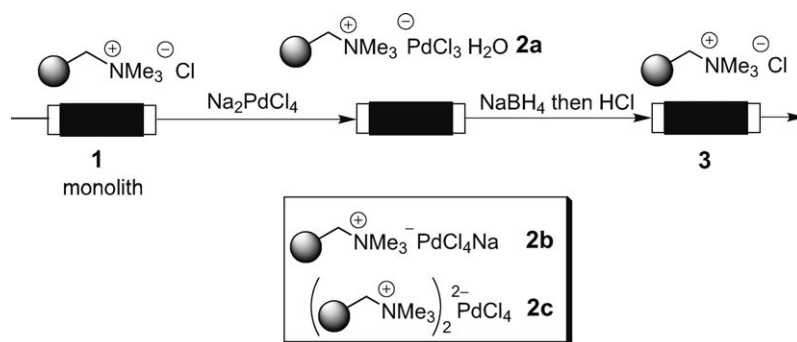
Generating Pd(0) species inside the PASSflow reactor is achieved by pumping an aqueous solution of sodium tetrachloropalladate (Na_2PdCl_4) through the PASSflow reactor loaded with anion exchange resin **1** (chloride form). This process leads to instantaneous ion exchange (Scheme 1). However, the stoichiometry of this process is not known as three possible species **2a–c** can be considered. Based on EPMA (electron probe microanalysis) and EDXS (energy dispersive X-ray spectroscopy) scanning profiles, which allowed us to determine both the palladium as well as chlorine profiles inside the polymer/glass composite material, we propose that ionic species **2a** is present on the ion

exchange resin (see Figs. S1 and S2 of Supporting Information).

Governing Factors for Pd Nanoparticle Size

As the Pd particle size will have a strong effect on the catalytic performance under classical thermal as well as microwave irradiating conditions, we first studied the influence of the flow rate during borohydride reduction inside the composite material on the palladium particle size. Loading resins at a low flow rate resulted in a shell-like distribution of palladate, whereas high flow rate leads to a uniform palladium distribution. The palladium distribution can be seen from the black colour in broken composite rings (Supporting Information; Figure S1). Taking advantage of the flow-through conditions with the composite Raschig rings inside the new reactor concept (Figure 1) reduction was performed under different flow conditions: a) pure diffusive operation (batch with shaking, no forced flow through the pore volume of the samples), b) an intermediate regime flow rate (10 mL min^{-1}) where external diffusion controls the process and c) pure kinetic conditions under flow operation (110 mL min^{-1}).

Reduction of the ion-exchanged palladate under flow conditions yielded smaller Pd clusters with a narrower particle size distribution and a better dispersion throughout the whole polymeric phase compared to reduction under diffusion control as judged by transmission electron microscopy (TEM) (Figure 2; Supporting Information; Figure S3) The fact that the average particle size did not decrease after increasing the flow conditions from 10 to 110 mL min^{-1} clearly reveals a smaller diffusion limitation for the borohydride than for the palladate anion. Consequently, a flow rate of 10 mL min^{-1} was chosen as standard protocol for all reduction procedures. Also the nature of the polymer composition has a pronounced influence on the Pd particle size.^[41] Thus, we prepared a set of polymers which differed in the degree of cross-linking (5.3, 10, 20 and 30% wt DVB). These were functional-



Scheme 1. Formation of Pd(0) nanoparticles inside the PASSflow reactor.

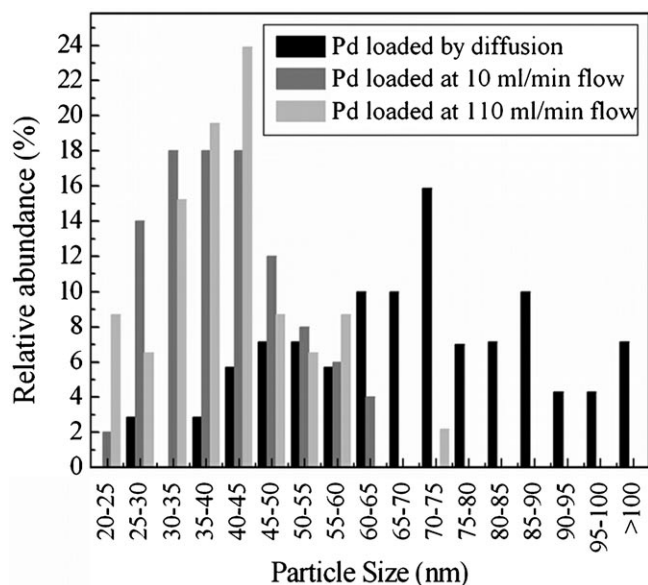


Figure 2. Pd cluster size distribution collected from TEM micrographs (see also Supporting Information; Figure S3) (polymer: VBC/DVB (5.3%)); loaded samples by diffusion based on 70 Pd particles; and loaded samples under flow conditions based on 50 Pd particles.

ized with Pd particles under flow conditions. Again, the cluster size distribution was analyzed by TEM (Figure 3). The particle sizes did not differ for samples containing 5.3 and 10% DVB, a small shift to smaller clusters was encountered for the 20% DVB sample and a large change can be noted when the degree of cross-linking was raised to 30% DVB.

With reference to a mathematical model,^[42] it can be assumed that during the precipitation polymerization process (Figure 1a) the polymeric particles grow from a starting nucleus to which polymeric layers are being added, leading to an onion-like shell structure with a decreasing gradient of cross-linking from the core to the outer shell. The observed lack of sensitivity to the content of cross-linker DVB between 5.3 and 10% wt, the small change in the 20% and finally, the pronounced shift in the 30% wt sample could in principle be ascribed to the particle morphology. Thus, a polymeric phase containing 30% DVB also has rigid spaces between polymer chains in the outer shell, preventing agglomeration and as a consequence leading to reduced Pd cluster size.

An additional four polymeric samples were prepared that differed in the density of cationic sites. We expected that site isolation will reduce the process of agglomeration of Pd particles upon formation as well during catalytic transformations. These samples were prepared by adding styrene to the mixture of monomers thereby gradually exchanging VBC by the inert spacer styrene. The molar ratio of styrene and VBC was 1:1, 10:1 and 30:1 (for detailed polymer composition see Supporting Information, Table S2). However, the properties of the polymeric samples with a high degree of cross-linking (30% DVB) were only further studied for the sample styrene/VBC 1:1 as TEM analyses for all other highly cross-linked samples turned out to be inconclusive, which hampered precise judgments.

Spacing the ion exchange sites in samples containing 5.3% DVB (styrene/VBC molar ratio from 0:1 to 1:1) results in dilution of the large Pd agglomerates

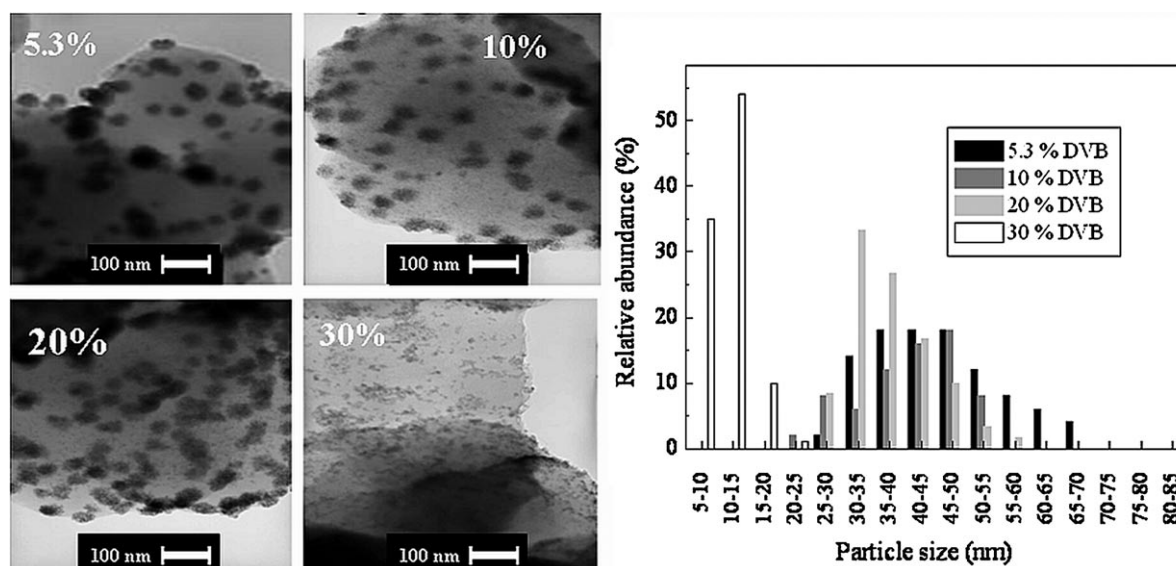


Figure 3. Left: TEM bright-field images of Pd clusters of different polymeric phases (5.3, 10, 20 and 30% DVB crosslinker) prepared under intermediate regime flow conditions. Scale bars indicate 100 nm. Right: Pd cluster size distribution based on 50 Pd clusters.

(clusters) in a less dense environment of individual Pd nanoparticles (see Figure 4). The TEM micrographs at higher magnification clearly reveal that the large Pd agglomerates are in fact a dense spherical packing of smaller Pd nanoparticles. This is particularly well documented for the “diluted” samples. For samples with 5.3% DVB, the increase of styrene content leads to larger distances between the ion exchange sites thereby resulting not only in the dilution of the small agglomerates but in an overall decrease of the Pd nanoparticle size as is shown in Figure 5.

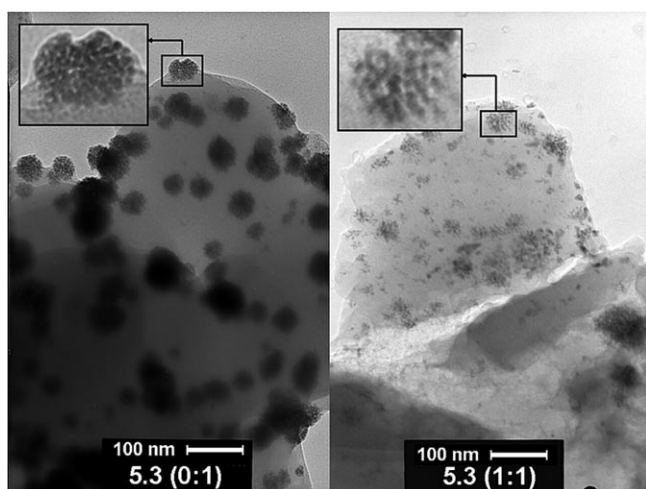


Figure 4. TEM micrographs of samples without styrene (*left*) and with a 1:1 molar ratio of styrene and VBC (*right*).

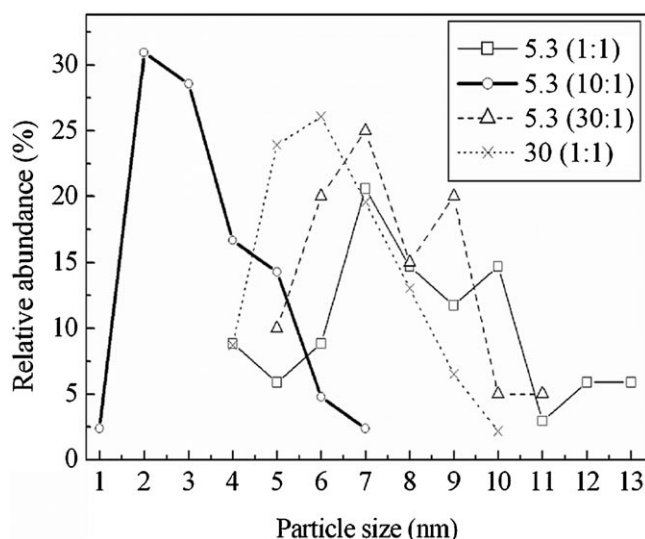


Figure 5. Pd cluster size distribution (based on 40 Pd particles) of samples with different styrene content collected from TEM pictures (see Supporting Information; Figure S6).

At this point a general trend can be drawn. By increasing the styrene content smaller clusters and smaller nanoparticles are generated.

Selective Heating Using Microwave Irradiation

The ability of a specific material to convert microwave energy into heat at a given frequency and temperature is determined by the so-called loss tangent ($\tan \delta$), expressed as the quotient, $\tan \delta = \epsilon''/\epsilon'$, where ϵ'' is the dielectric loss, indicative of the efficiency with which electromagnetic radiation is converted into heat, and ϵ' is the dielectric constant, describing the ability of molecules to be polarized by the electric field.^[36] A reaction medium with a high $\tan \delta$ at the standard operating frequency of a microwave reactor (2.45 GHz) is required for good absorption and, consequently, for efficient heating. As indicated above our reactor design should in principle allow for the selective heating of the strongly microwave absorbing^[36] palladium nanoparticles by microwave energy, since both the chosen reactor material (PEEK) as well as the porous glass polymer composite Raschig rings should be microwave transparent. In order to verify this hypothesis we have conducted an extensive set of microwave irradiation experiments with all the materials used in the reactor construction. The difference in the microwave absorbance of the various composite materials was readily demonstrated by comparing heating profiles when suspended in a microwave transparent solvent^[36] such as carbon tetrachloride. For these experiments carried out in a batch microwave reactor, a fully microwave transparent quartz reaction vessel and an accurate internal fiber-optic temperature probe was utilized.^[43] Exposure of a stirred sample of carbon tetrachloride to 100 W constant magnetron output power for 5 min led to virtually no detectable heating of the solvent (Figure 6, curve a). A small heating effect raising the bulk temperature of the mixture was seen under identical conditions for a sample of PEEK suspended in the microwave transparent solvent (curve b), and for one of the standard glass Raschig rings (without polymer and Pd) displayed in Figure 1 b (curve c), confirming the more or less microwave transparent nature of the base reactor materials. In contrast, a suspension of one monolithic glass/polymer composite Raschig ring possessing anion exchange functionality [that is, **1**, Figure S1 in Supporting Information (VBC, 5.3 wt% DVB)] demonstrated significant absorbance of microwave energy and conversion into heat (curve d), probably as a result of the ionic character of the polymer matrix, invoking an ionic conduction heating mechanism.^[36] Importantly, however, under the same conditions the palladated Raschig rings **3** proved to be strongly microwave absorbing raising the bulk temperature of

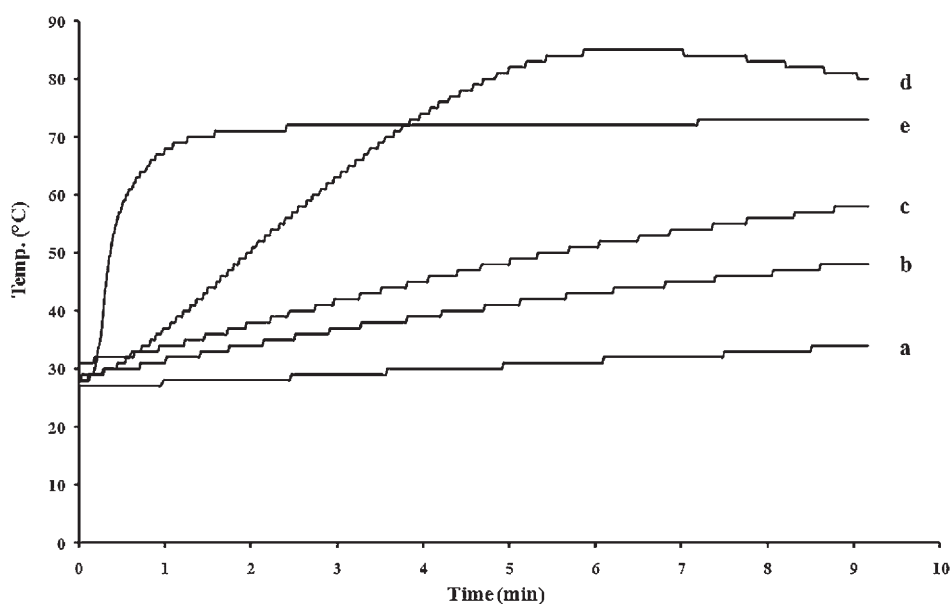


Figure 6. Microwave heating profiles for materials suspended in carbon tetrachloride. Experiments were carried out using a single-mode microwave instrument in a 10 mL sealed quartz vessel with magnetic stirring (fiber-optic temperature measurement) using 100 W constant magnetron power output for 5 min. Profile **a**: pure carbon tetrachloride. Profile **b**: PEEK sample suspended in carbon tetrachloride. Profile **c**: one glass Raschig ring (cf. Figure 1 b) suspended in carbon tetrachloride. Profile **d**: glass/polymer composite **1** (5.3% DVB, 1:1 styrene/VBC) suspended in carbon tetrachloride. Profile **e**: palladated glass/polymer composite **3** (5.3% DVB, 1:1 styrene/VBC) suspended in carbon tetrachloride.

the microwave transparent solvent from room temperature to 70 °C within about one minute of irradiation (curve e). This dramatic heating effect is clearly the consequence of the selective absorbance of microwave irradiation by the metal particles on the polymeric support. It should be stressed that the measured temperature of *ca.* 70 °C merely reflects the bulk temperature of the solvent and not the intrinsic temperature localized around the palladium particles which may be significantly higher.

We have additionally recorded the heating profiles for two other solvents under constant 100 W microwave irradiation conditions, namely for the weak microwave absorber toluene ($\tan \delta = 0.040$) and the strong absorber ethanol ($\tan \delta = 0.941$). As expected, toluene proved to be significantly less microwave absorbing than the palladated Raschig ring/carbon tetrachloride suspensions, whereas ethanol was significantly stronger absorbing (data not shown).

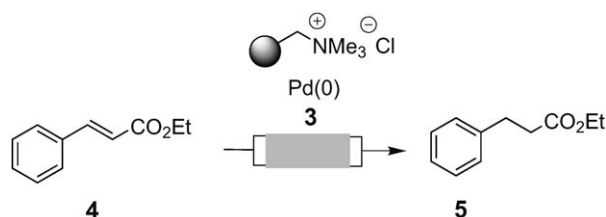
Catalytic Transfer Hydrogenations

Having established the factors that govern the distribution on the polymeric phase and the particle diameter of palladium particles, as well as having studied the suitability of the PASSflow reactor under microwave irradiating conditions, we focussed on the catalytic performance of these nanoparticles. Although we have shown that these Pd nanoparticles show excel-

lent activity in C–C cross-coupling reactions,^[31] we tried to keep the set-up simple thus avoiding the use of two organic coupling partners. Therefore, in the present study, the transfer hydrogenation of ethyl cinnamate **4** to dihydrocinnamate **5** served as benchmark reaction (Table 1). In principal, four modes of conducting this transformation were studied in detail which are transfer hydrogenations at 70 °C with a) thermal heating as well as b) MW irradiation in a batch wise operation and continuous flow hydrogenations again with c) thermal as well as d) MW irradiation. In this context, it is of importance to understand how the nature and local environment of the Pd(0) particle on the polymer support is correlated with its reactivity and thus affects the efficiency of the hydrogenation process under the four differing process conditions. As a result a correlation between the metal particle size (before and after several runs) and the efficiency of the hydrogenation can be drawn. Furthermore, the undoubtedly important role of the solvent under MW irradiation was investigated.

In the initial experiment the transfer hydrogenation was carried out under batch as well as continuous flow conditions [0.072 M **4** in EtOH/cyclohexene (1:1), 70 °C; flow rate = 2 mL min⁻¹ for flow through mode] using Raschig rings with a polymeric composition of 5.3% DVB as cross-linker and only VBC as major second monomer. The flow-through reaction was carried out with glass/polymer composite rings which were incorporated into a type of PASSflow re-

Table 1. Transfer hydrogenation of ethyl cinnamate under batch and continuous flow conditions at 70 °C bulk temperature (5.3% DVB, VBC; palladate loading and reduction were conducted under two different conditions: sole diffusion and kinetic regime).



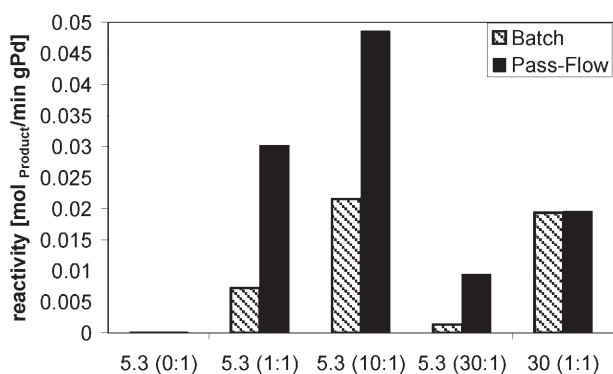
Batch/flow mode	Solvent	Reaction time (h) until full transformation		
		Pd loading by pure diffusion, conventional heating	Pd loading at a flow rate of 10 mL min ⁻¹ , conventional heating	Pd loading by pure diffusion, MW
Batch	EtOH/cyclohexene	14 h	14 h	3.25 h
Flow	EtOH/cyclohexene	14 h	3 h	3.75 h
Batch	Tol/cyclohexene	2 h	2 h	3.75 h
Flow	Tol/cyclohexene	24 h	48 h	4.5 h

actor shown in Figure 1c. In Figure 7a (conventional heating) ten experiments are depicted, which were carried out under identical conditions except that five different composite materials were employed. The results are normalized with respect to the Pd content of the samples (see Supporting Information; Figure S7). They clearly demonstrate that the catalyst activity changes with the nature of the polymeric phase which itself determines the Pd cluster and particle size (see also Figure 5) In essence, dilution of the Pd clusters with respect to the individual nanoparticles by adding styrene as a spacer monomer enhances the reactivity independent from the flow method (e.g., compare double column 1 with double column 2 in Figure 7a). Furthermore, the smaller the Pd particle size the higher the reactivity of the catalyst in these transfer hydrogenations regardless of whether batch or continuous flow conditions are employed (e.g., compare double column 2 with 3 in Figure 7a). As a general trend in heterogeneous catalysis this fact is expected in terms of the great increase in the specific catalytic active surface area of Pd. Additionally, continuous flow commonly results in better performance compared to batch mode hydrogenations due to the increase in the mass transfer processes of the reactants. The relationship between Pd particle size and reactivity is similar when transfer hydrogenations were conducted in toluene although transfer hydrogenation proceeds more efficiently in ethanol (Figure 7b). When switching from conventional to microwave heating transfer hydrogenations at 70 °C (measured

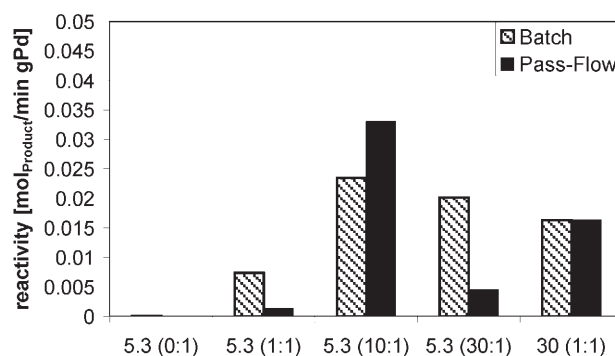
bulk temperature) perform better under continuous flow conditions than in the batch mode (Figure 7c and Figure 7d). Now, polymeric backbones that accommodate larger Pd nanoparticles show better catalytic reactivity compared to those that are loaded with smaller ones. However, the trends noted for the experiments conducted with conventional heating prevail in the same manner, namely that continuous flow conditions give better results for transfer hydrogenations than the batch mode and that ethanol is the solvent of choice in comparison to toluene. Importantly, Figure 7a-d clearly reveal that microwave irradiation leads to an improved performance irrespective of the Pd-doped polymeric sample employed and irrespective of whether the hydrogenation is performed in batch or flow mode. Again, we would like to stress that here conventional and microwave heating results are difficult to compare as far as the genuine “reaction temperature” is concerned due to the selective heating of the metallic nanoparticles by microwaves.^[39,40]

The inversion in the reactivity pattern with respect to particle size and heating method already described could be associated with the special characteristics of a microwave irradiated process. Employing microwave dielectric heating, the power converted to heat in an irradiated particle is proportional to the volume of the particle^[44] whereas the heat transferred from a particle to the environment is proportional to the heat exchange surface area. Hence, bigger particles have a bigger volume to surface area ratio than small-

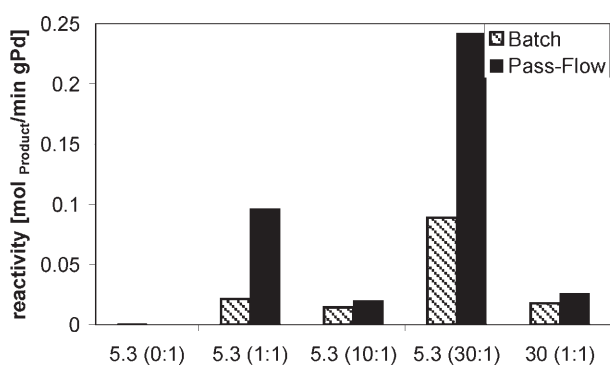
a) Conventional heating (in EtOH)



b) Conventional heating (in toluene)



c) Microwave heating (in EtOH)



d) Microwave heating (in toluene)

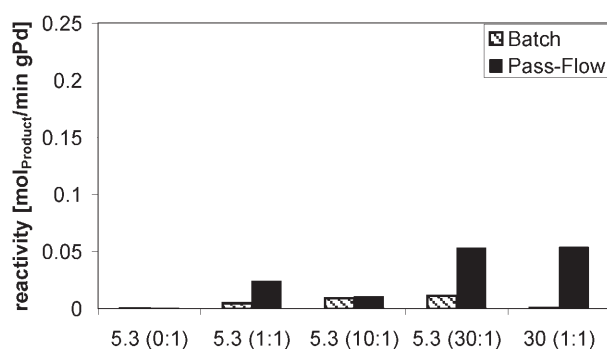


Figure 7. Transfer hydrogenations of ethyl cinnamate (**4**) in batch as well as flow mode (refer to Table 1; abscissa: for example, 5.3 (1:1) refers to a polymeric sample composed of 5.3% DVB cross-linker and a 1:1 ratio of VBC and styrene). Reactivity profiles (mol product/min g Pd) of different Pd(0)-doped polymeric phases in transfer hydrogenations of cinnamate **4**. Figure 7a and Figure 7b refer to conventional heating (70°C) in batch as well as flow mode in ethanol and toluene, respectively. Figure 7c and Figure 7d refer to the corresponding set of experiments under MW irradiation conditions (bulk temperature 70°C).

er particles, thereby increasing the heat accumulated in the particles and as a result providing a hypothetical higher hot spot effect. Such an effect, which has not been possible until now to be theoretically modelled,^[39] is under current investigation in our laboratories.

Reusability Studies and Aging

a) Reusability Study

Having established the performance of individual Pd-doped polymer samples under different conditions, we then investigated the reusability of these catalyst samples, starting with batch operations. Conditions were maintained as described in the section “Catalytic Transfer Hydrogenations” and the results for up to ten runs are summarized in Figure 8a to d. Using ethanol as solvent (Figure 8a) results in an improved re-

usability of the catalytic samples with a high palladium content. However, samples with low palladium loading are deactivated rather rapidly (curves highlighted with arrows). The same trend is observed with toluene as solvent (Figure 8b) even though deactivation only occurs after more runs (curves highlighted with arrows). A different behaviour was observed under microwave irradiating conditions. All samples displayed a stable performance over ten runs in ethanol as well as in toluene. The behaviour of the non-diluted sample 5.3 (0:1) is out of this general trend, since a clear deactivation is observed after the sixth run. This might be explained by the higher energy conversion stress suffered by the Pd particles, since in a non-microwave absorbing solvent all the heat to reach the desired bulk temperature comes from the conversion of the whole power input solely absorbed by the Pd particles.

Deactivation of noble metal-supported heterogeneous catalysts can occur by a) sintering of metal crys-

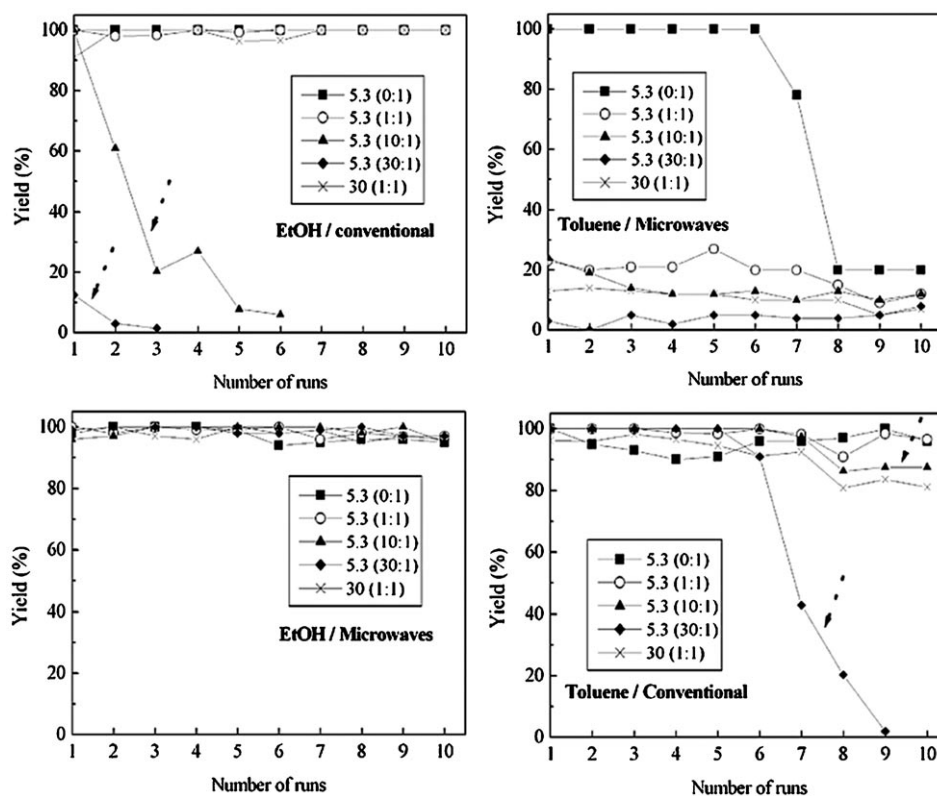


Figure 8. Performance of Pd-doped polymers after repeated transfer hydrogenations of **4** (batch mode).

tallites, b) formation of side products which poison the metal surface, c) chemical changes involving the metal (e.g., oxidation, leaching) and d) chemical and physicochemical changes involving the support. Kralik et al. reported a possible deactivation caused by the combination of the hydrogenolysis of the polymer backbones and a Pd leaching process.^[45] In the present case, degradation of the polymeric phase can be neglected. In addition, formation of poisoning side products has never been reported for this kind of transfer hydrogenations. The amount of leaching of Pd was analyzed for all batch experiments (thermal and microwave heating) and all flow-through experiments (thermal conditions). We commonly collected samples after the 5th run for determining the degree of Pd leaching by ICP-MS. We found that leaching was commonly very low (between 0.002 and 0.1% Pd) with reference to the amount of Pd initially employed (see Supporting Information; Table S4).

Therefore, we also conducted analytical studies on determining Pd particle size changes after catalysis utilizing STEM analysis. In Figure 9 a comparison between fresh samples (5.3% DVB; 0:1) of composite material and the aged samples after the tenth run (both heating methods in ethanol) are depicted. A slight increase in the cluster size can be observed for the sample which had been heated under conventional conditions, while almost no agglomeration was found in the sample which had been heated under mi-

crowave irradiating conditions. The fact that no catalytic activity loss was found for the same sample indicates that no sintering of metal crystallites had occurred.

b) Aging of Nanoparticles

Commonly, fresh Raschig rings contain Pd particles which slightly differ in size, depending how loading was performed (diffusive 4–5 nm; convective 6 nm). When transfer hydrogenations were performed under batch conditions the particles did not change in size, even not after the 10th run. Only the agglomerates slightly increase during the catalytic process. MW irradiation leads to a slight increase of average Pd particle size after the 10th run (diffusive 6 nm; convective 6–10 nm). In contrast to Pd particles that have been loaded under convective conditions, the diffusively loaded samples show substantial increases in particle as well as cluster size. This can be ascribed to the fact that the Pd particles are almost exclusively located in the outer sphere of the Raschig rings when diffusion controlled loading had been conducted (see Figure S1 in Supporting Information) which leads to higher local concentrations. In contrast, loading under convective flow conditions leads to more even distribution throughout the rings. Changes in particle as well as cluster size during transfer hydrogenation are mar-

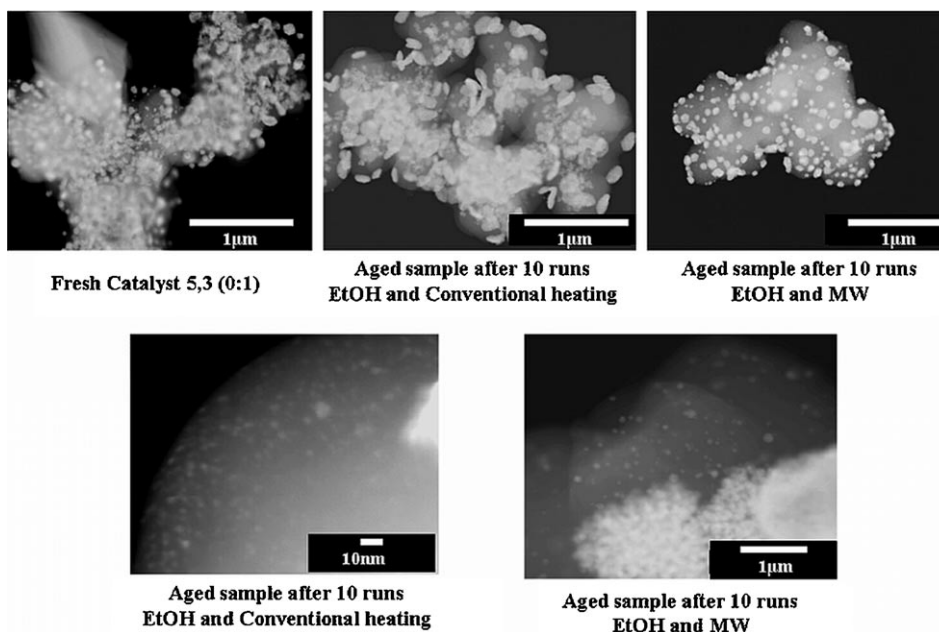


Figure 9. Dark-field STEM pictures of the non-diluted composite before hydrogenation and after 10 runs.

ginal irrespective of whether toluene or ethanol serves as solvent.

The current data do not give a conclusive and homogeneous picture. However, the following trends can be summarized: a) Higher degrees of cross-linking lead to Pd species with lower catalytic activity. This, however, results in glass-polymer composite materials that show prolonged activity. b) In contrast, polymers with smaller degrees of cross-linking or higher dilution of Pd particles on their surfaces (using styrene as third monomeric component) show higher catalytic activity which more rapidly erode with each run.

Conclusions

In summary, it was demonstrated that the PASSflow technique can be successfully utilized in a catalytic process using transition metal catalysts. This study reveals that this technique can be extended to microwave heated operations. The influence of catalyst distribution inside the composites was investigated for the transfer hydrogenation of ethyl cinnamate as a model reaction. It was observed that the reactivity of the catalysts prepared is different in traditional compared to microwave heating. The reason for the different performance is related to the presence of two effects. On one hand a high active site dilution produces a decrease in the nanoparticle size leading to a higher surface area and coupled with this to a higher catalytic activity. On the other hand the same dilution produces a decrease in the Pd content of the catalysts leading to a small rate enhancement by hot spot ef-

fects. At low Pd content the amount of microwave energy that can be absorbed and dissipated by the catalyst drops. However, an inversion of the reactivity with the particle diameter changing from traditional heating to microwave heating was observed. That means that smaller particles are more active in traditional heating whereas bigger particles perform better in microwave heating. This can be explained by hot spot effects which depend on the particle diameter. The bigger the size, the higher the possible temperature gradient between particle and bulk liquid becomes.^[46] A different behaviour from the aspect of catalyst reusability was observed for different heating methods. Low to intermediate active site dilution is beneficial if the catalyst is conventionally heated. Under microwave heated samples no loss of catalytic activity was found.

Flow chemistry in conjunction with microwave heating is still in its infancy.^[47] Because of the limited penetration depth of microwave irradiation into absorbing media, the scale-up of microwave-assisted reactions is inherently problematic using conventional batch processing. Using microwaves, the solution to the scale-up problem therefore has to involve a flow process and we are currently exploring different strategies realizing this process.

Experimental Section

General Methods

TEM measurements were conducted on a Philips CM 200 microscope at 200 kV. STEM micrographs were recorded on

a JEOL JEM-2100F-UHR microscope at 200 kV in HAADF contrast. Samples were collected after crushing composite Raschig rings into fine powder, dispersion of the material in a volatile liquid (ethanol) and finally subjecting it to a fine mesh carbon net which is electron transparent. EPMA-EDXS scanning was carried out with a Cameca SX 100 Microprobe analyser which had a Cambridge CS44 SEM camera incorporated in combination with an EDAX spectrometer. Ion exchange measurements of palladate were achieved by UV-VIS spectroscopy of the palladate solution using a Hach DR 4000V Spectrophotometer (430 nm wavelength). NMR spectra were recorded with a Bruker DPX-400 spectrometer at 400 MHz (^1H NMR) and at 125 MHz (^{13}C NMR) in CDCl_3 using tetramethylsilane as the internal standard. Mass spectra (EI) were obtained at 70 eV with a type VG Autospec apparatus (Micromass). GC analyses were conducted using a Hewlett-Packard HP 6890 Series GC System equipped with a SE-54 capillary column (25 m, Macherey-Nagel) and a FID detector 19231 D/E. Flash column chromatography was performed on Merck silica gel 60 (230–400 mesh). Commercially available reagents and dry solvents were used as received. All reactions were carried out in a continuous flow apparatus from Chelona GmbH, Potsdam.

Reactor Concept

Rings are aligned on a perforated tube inside the reactor. The spaces between the rings were sealed with KALREZ® or VITON® polymer. These gaskets prevent bypass. The whole structure forces the fluid to flow from an annular gap through the ring walls and leaving the reactor through the perforated inner tube. For a detailed description see ref.^[33]

Composite Materials

All samples that were prepared without the use of styrene as monomer were obtained by copolymerization of vinylbenzyl chloride (VBC, 90% purity), in the presence of divinylbenzene (DVB, 65% purity) as cross-linking monomer (5.3 to 30% wt) using precipitation polymerization inside a fractal porous Raschig ring. In contrast, all catalysts that also contain styrene as monomer were prepared by altering the above-mentioned procedure by additionally adding styrene (99% purity) to the polymerization mixture. The amount in mass percent and mol percent used for the preparation of the different polymerization mixtures are listed in Table 1 of the Supporting Information. All polymer samples obtained by precipitation polymerization were functionalized in the following by amination with triethylamine in toluene which afforded the corresponding polymers functionalized with quaternary ammonium chloride sites.

Palladium Loading Procedures

Batch procedure: Raschig rings (100 g; 5.3% DVB, loading = 0.17 mmol/ring) were washed with 2N HCl (510 mL) for 0.5 h and water until the eluent showed pH 7. Then the Raschig rings were shaken in a 0.03 M solution of sodium tetrachloropalladate (5 g, 15.3 mmol) in water under N_2 (O_2 exclusion) atmosphere until the colour of the solution had turned from red to yellow. The rings were washed with water (1.7 L) until no palladate salts leave the rings any-

more. Reduction was achieved by addition of a solution of 0.2 M NaBH_4 (6 g, 158.6 mmol) in water until gas evolution stopped. The rings were washed with water (500 mL) and methanol (500 mL) before gently shaking them in a solution of 2N HCl (510 mL). After washing the rings with water (until pH 7) and methanol the rings are dried in high vacuum.

Flow procedure: Loading under flow conditions was typically carried out by incorporation of five Raschig rings inside a stainless steel PASSflow reactor (reactor set-up depicted in Figure 1c). The palladate ion exchange was optimized at different flow rates (10–110 mL). The graphic that describes the initial rate of ion exchange vs. flow rate reveals that at 110 mL min^{-1} the ion exchange rate is no longer dependent on the flow rate (Supporting Information). As a result under these flow conditions external diffusion can be neglected. The loading procedures for preparing the various catalyst samples were conducted stepwise. For the polymeric samples that are composed of 5.3%, 10%, 20% and 30% DVB (styrene/VBC = 0:1) and 5.3% DVB (styrene/VBC = 1:1) ion exchange was achieved within 2 h by circulating an aqueous solution (0.028 M; 1:1 ratio ion exchange capacity and palladate) of $\text{Na}_2\text{Cl}_4\text{Pd}\cdot 3\text{H}_2\text{O}$ (refer also to Table 1 of the Supporting Information) through the reactor. Except for the kinetic studies, the flow rate was kept at 10 mL min^{-1} . In the following, the reactor was flushed for one hour with distilled water at a flow rate of 5 mL min^{-1} before a solution of borohydride in water (1.5 g, 39.65 mmol; 200 mL) was pumped through the PASSflow reactor at a flow rate of 10 mL min^{-1} (except for the kinetic studies). The loading was terminated by three washing steps: (a) distilled water, 1 h, 5 mL min^{-1} ; (b) 100 mL 2M HCl, 9 mL min^{-1} and (c) distilled water, 9 mL min^{-1} until the pH at the outlet was determined to be 7. For the polymeric samples that are composed of 5.3% DVB (styrene/VBC = 10:1) and 30% (1:1) the loading procedure was as follows: (a) ion exchange within 2 h by circulating (10 mL min^{-1}) a solution of THF/water (0.028 M; 1:1 ratio ion exchange capacity and palladate) of $\text{Na}_2\text{Cl}_4\text{Pd}\cdot 3\text{H}_2\text{O}$; (b) THF/water, 1 h, 5 mL min^{-1} ; (c) borohydride solution in THF/water (0.75 g, 20 mmol; 100 mL), 10 mL min^{-1} ; (d) THF/water, 1 h, 5 mL min^{-1} ; (e) 11 mL 2M HCl in 100 mL THF/water, 9 mL min^{-1} and finally (f) rings washed in batch with a mixture THF/water for 12 h. As solvent mixtures THF/water (3:1) for the samples 5.3% DVB (styrene/VBC = 10:1) and THF/water (1:3) for the sample 30% DVB (styrene/VBC = 1:1) turned out best suited.

Transfer Hydrogenation in Batch and Continuous Flow Modes under Conventional Heating

Batch Mode: In a typical experiment a 10-mL reaction vessel was filled with 5 mL of the appropriate solvent mixture EtOH:cyclohexene = 1:1 or toluene:cyclohexene = 1:1, two palladated Raschig rings **3** (Table 1; Supporting Information) and 60 μL (0.36 mmol) of ethyl cinnamate under nitrogen. The vial was heated to 70°C and shaken. After the time listed in Table 1, the rings were removed by filtration, rinsed with ethyl acetate and the combined organic phases were removed under reduced pressure. Typically, a colourless oil (yield: 64 mg; 100%) was collected. The rings were

dried under reduced pressure and stored under nitrogen atmosphere.

Continuous Flow: The PASSflow reactor (Figure 1c) was charged with three palladated Raschig rings **3** (Table 1), and connected to the HPLC pump. A freshly prepared mixture of EtOH:cyclohexene or toluene:cyclohexene (50 mL, 1:1) was used as a stock solution. Initially, the pump was primed by injecting this reaction solvent mixture while maintaining a flow rate of 2 mL min⁻¹. During the period of flow stabilization, the PASSflow reactor was checked for leakage and kept outside of the oven. The reactor was subsequently introduced into the oven while the pumping of solvent flow is stopped. Thereafter, the inlet was switched to the actual reaction mixture of EtOH:cyclohexene or toluene:cyclohexene (14 mL, 1:1), containing 90 μ L (0.53 mmol) of ethyl cinnamate, while maintaining a flow rate of 2 mL min⁻¹ (reaction times are listed in Table 1). An aliquot sample was taken and the degree of transfer-hydrogenation was determined by GC-analysis. The reactor was washed with the solvent mixture (20 mL) and the product was collected after removal of the combined solvents under reduced pressure. Prior to the next reaction the PASSflow reactor was washed by switching the inlet to a reservoir with EtOAc for 10 min and then to the reservoir with the reaction solvent mixture without ethyl cinnamate for another 10 min.

Spectroscopic Data for Ethyl Dihydrocinnamate **5**

¹H NMR (200 MHz, CDCl₃, CDCl₃ = 7.26 ppm): δ = 7.28 (m, 5H, 2-H, 6-H), 4.16 (q, J = 7.1 Hz, 2H, 10-H), 2.99 (t, J = 8.1 Hz, 2H, 7-H), 2.66 (t, J = 8.1 Hz, 8-H), 1.27 (t, J = 7.1 Hz, 3H, 11-H); ¹³C NMR (100 MHz, CDCl₃, CDCl₃ = 77.36 ppm): δ = 173.2 (q, C-9), 140.8 (q, C-1), 128.7 (t, C-2, C-6), 128.6 (t, C-3, C-5), 126.5 (t, C-4), 60.7 (s, C-10), 36.2 (s, C-8), 31.3 (s, C-7), 14.5 (p, C-11); GC-MS(EI): m/z (%) = 178 (20) [M⁺].

Microwave Experiments

All microwave experiments were performed with a single-mode CEM Discover/Voyager microwave instrument at 2450 MHz controlled irradiation, using standard Pyrex vials, custom-made high purity quartz vessels or the appropriate PASSflow reactor (Figure 1c). The temperature profiles of the solvents were monitored by using a fibre-optic probe. When performing PASSflow experiments the fiber-optic probe was mounted on the outside wall of the PASSflow reactor with a thin TeflonTM tape. To maintain stable power and temperature during the reaction, the microwave cavity and outside surface of the PASSflow reactor was actively cooled by compressed air to remove latent heat. It should be noted that it was only possible to monitor the temperature of the outside reactor wall corresponding roughly to the temperature of the bulk reaction mixture and not the actual temperature near the metal particles inside the reactor.

Heating Profiles of Materials/Solvents (Figure 6)

In a typical experiment a 10-mL quartz reaction vessel containing a magnetic stir bar was filled with 5 mL of the appropriate solvent (CCl₄, EtOH, toluene) or solvent/material mixture. The vial was closed and irradiated with 100 W con-

stant magnetron output power for 5 min. The fibre-optic probe was introduced into the reaction vessel protected by a sapphire immersion well. When obtaining the temperature profiles of the solid materials only CCl₄ was employed as solvent media. The experiments were performed as described above by adding one piece of: PEEK, Raschig rings, polymer composite **1** and polymer composite **3** (5.3% DVB, 1:1 styrene/VBC).

Transfer Hydrogenation in Batch and Continuous-Flow under Microwave Irradiation

Batch Mode Microwave Processing: In a typical experiment a 10-mL Pyrex reaction vessel was filled with 5 mL of the appropriate solvent mixture EtOH:cyclohexene = 1:1 or toluene:cyclohexene = 1:1, two palladated Raschig rings **3** (Table 1; Supporting Information) and 60 μ L of ethyl cinnamate. The vial was subsequently sealed and irradiated for 30 min at a set temperature of 70°C (IR control) and constant stirring of the mixture. After 30 min, an aliquot sample was taken and the degree of transfer hydrogenation determined by HPLC-analysis at 215/254 nm.

Continuous Flow Microwave Processing: The PASSflow reactor (Figure 1c) was charged with two palladated Raschig rings **3** (Table 1), tightened and connected to the CEM Voyager module and HPLC pump. A freshly prepared mixture of EtOH:cyclohexene or toluene:cyclohexene (50 mL, 1:1) was used as a stock solution. Initially, the pump is primed by injecting this reaction solvent mixture while maintaining a flow rate of 2 mL min⁻¹. During the period of flow and back pressure stabilization, the PASSflow reactor is checked for leakage and kept outside of the microwave cavity. The reactor is subsequently introduced into the cavity while the pumping of solvent flow is stopped. Thereafter, the reaction parameters (60°C, 30–50 W magnetron power, 2 min ramp time and 180 min hold time) are loaded and the inlet is switched to the actual reaction mixture of EtOH:cyclohexene or toluene:cyclohexene (13 mL, 1:1), containing 90 μ L of ethyl cinnamate, while maintaining a flow rate of 2 mL min⁻¹. The flow is maintained in a closed loop (the outlet is introduced into the reaction mixture reservoir) for 180 min. An aliquot sample was taken and the degree of transfer-hydrogenation was determined by HPLC analysis at 215/254 nm. Prior to the next reaction the PASSflow reactor was washed by switching the inlet to a reservoir with EtOAc for 10 min and then to the reservoir with the reaction solvent mixture without ethyl cinnamate for another 10 min. For a picture of the reactor set-up refer to the Supporting Information.

Stability/Reactivity Studies

Microwave conditions for batch and continuous flow experiments were used as described above. A matrix of ten runs in sequence was performed with all six types of palladated Raschig rings **3** under batch as well as under continuous flow conditions. The degree of transfer-hydrogenation was determined by HPLC-analysis at 215/254 nm.

Kinetic Studies with Palladated Raschig Rings

Thermal conditions for batch and continuous flow experiments were used as described above. An aliquot sample was

taken at periods of 30 min reaction time until the transfer hydrogenation was complete or no further improvement of the conversion could be monitored. The degree of transfer hydrogenation was determined by GC analysis.

Acknowledgements

Financial support for this work was given by the DFG (grant Ki 397/6-1 and KU 853/3-1), the Austrian Science Fund (FWF, grant I18-N07), the Fonds der Chemischen Industrie and in part by the Max-Buchner-Stiftung for which we are grateful.

References

- [1] a) D. Astruc, F. Lu, J.R. Aranzaes, *Angew. Chem.* **2005**, *117*, 8062–8083; *Angew. Chem. Int. Ed.* **2005**, *44*, 7852–7872; b) V. Farina, *Adv. Synth. Catal.* **2004**, *346*, 1553–1582; c) N. T. S. Phan, M. van der Sluys, C. W. Jones, *Adv. Synth. Catal.* **2006**, *348*, 609–679.
- [2] a) L. Djakovitch, M. Wagner, C. G. Hartung, M. Beller, K. Köhler, *J. Mol. Catal. A: Chem.* **2004**, *219*, 121–130; b) A. Biffis, M. Zecca, M. Basato, *J. Mol. Catal. A: Chem.* **2001**, *173*, 249–274; c) A. F. Schmidt, L. V. Mаметова, *Kinet. Catal.* **1996**, *37*, 406–408; d) A. Wali, S. M. Pillai, V. K. Kaushik, S. Satish, *Appl. Catal. A: General* **1996**, *135*, 83–93; e) F. Zhao, M. Arai, *React. Kinet. Catal. Lett.* **2004**, *81*, 281–289; f) A. Biffis, M. Zecca, M. Basato, *Eur. J. Inorg. Chem.* **2001**, 1131–1133.
- [3] a) J. P. M. Niederer, A. B. J. Arnold, W. F. Hölderich, B. Spliethoff, B. Tesche, M. T. Reetz, H. Bönemann, *Top. Catal.* **2002**, *18*, 265–269; b) N. Toshima, Y. Shiraishi, T. Teranishi, M. Miyake, T. Tominaga, H. Watanabe, W. Brijoux, H. Bönemann, G. Schmid, *Appl. Organomet. Chem.* **2001**, *15*, 178–196; c) M. T. Reetz, H. Schulenburg, M. Lopez, B. Spliethoff, B. Tesche, *Chimia* **2004**, *58*, 896–899.
- [4] a) C. P. Mehnert, D. W. Weaver, J. Y. Ying, *J. Am. Chem. Soc.* **1998**, *120*, 12289–12296; b) C. P. Mehnert, *Chem. Commun.* **1997**, 2215–2216; c) L. Djakovitch, K. Köhler, *J. Am. Chem. Soc.* **2001**, *123*, 5990–5999; d) R. G. Heidenreich, J. G. E. Krauter, J. Pietsch, K. Köhler, *J. Mol. Catal. A: Chem.* **2002**, *182–183*, 499–509; e) K. Köhler, R. G. Heidenreich, J. G. E. Krauter, J. Pietsch, *Chem. Eur. J.* **2002**, *8*, 622–631; f) K. Okumura, K. Nota, K. Yoshida, M. Niwa, *J. Catal.* **2005**, *231*, 245–253; g) L. Artok, H. Bulut, *Tetrahedron Lett.* **2004**, *45*, 3881–3884; h) S. Mandal, D. Roy, R. V. Chaudhari, M. Sastry, *Chem. Mater.* **2004**, *16*, 3714–3724; i) K. Köhler, W. Kleist, S. S. Pröckl, *Inorg. Chem.* **2007**, *46*, 1877–1883.
- [5] a) M.-C. Daniel, D. Astruc, *Chem. Rev.* **2004**, *104*, 293–346; b) M. Brust, M. Walker, D. Bethell, D. J. Schiffrin, R. Whyman, *J. Chem. Soc., Chem. Commun.* **1994**, 801–802; c) D. I. Gittins, F. Caruso, *Angew. Chem.* **2001**, *113*, 3089–3092; *Angew. Chem. Int. Ed.* **2001**, *40*, 3001–3004.
- [6] a) M. T. Reetz, W. Helbig, *J. Am. Chem. Soc.* **1994**, *116*, 7401–7402; b) M. T. Reetz, S. A. Quaiser, *Angew. Chem. Int. Ed. Eng.* **1995**, *34*, 2240–2241; *Angew. Chem.* **1995**, *107*, 2461–2463; c) M. T. Reetz, R. Breinbauer, K. Wanninger, *Tetrahedron Lett.* **1996**, *37*, 4499–4502; d) M. T. Reetz, G. Lohmer, *Chem. Commun.* **1996**, 1921–1923.
- [7] a) *Nanoparticles*, (Ed.: G. Schmid), Wiley-VCH, Weinheim, **2004**; b) R. G. Finke, in: *Metal Nanoparticles. Synthesis Characterization and Applications*, (Eds.: D. L. Feldheim, C. A. Foss Jr.), Marcel Dekker, New York, **2002**, chap. 2, p 17; c) *Nanoparticles and Nanostructured Films. Preparation, Characterization and Applications*, (Ed.: J. H. Fendler), Wiley-VCH, Weinheim, **1998**; d) G. Schmid, in: *Nanoscale Materials in Chemistry*, (Ed.: K. J. Klabunde), Wiley-Interscience, New York, **2001**, p 15.
- [8] Recent reviews on catalytic applications: a) M. A. El-Sayed, *Acc. Chem. Res.* **2001**, *34*, 257–264; b) R. M. Crooks, M. Zhao, L. Sun, V. Chechik, L. K. Yeung, *Acc. Chem. Res.* **2001**, *34*, 181–190; c) T. Yonezawa, N. Toshima, *Polymer-Stabilized Metal Nanoparticles: Preparation, Characterization and Applications*: in: *Advanced Functional Molecules and Polymers*, (Ed.: H. S. Nalwa), Accelerated Development, **2001**, chapter 3, p 65; d) A. B. R. Mayer, *Polym. Adv. Technol.* **2001**, *12*, 96–106; e) H. Bönemann, R. Richards; *Synth. Methods Organomet. Inorg. Chem.* **2002**, *10*, 209–224; f) A. Roucoux, J. Schulz, H. Patin, *Chem. Rev.* **2002**, *102*, 3757–3778; g) M. Moreno-Manas, R. Pleixats, *Acc. Chem. Res.* **2003**, *36*, 638–643; h) B. F. G. Johnson, *Top. Catal.* **2003**, *24*, 147–159.
- [9] X.-D. Mu, D. G. Evans, Y. Kou, *Catal. Lett.* **2004**, *97*, 151–154.
- [10] P. Claus, A. Brückner, C. Möhr, H. Hofmeister, *J. Am. Chem. Soc.* **2000**, *122*, 11430–11439.
- [11] A.-I. Kozlov, A. P. Kozlova, K. Asakura, Y. Matsui, T. Kogure, T. Shido, Y. Iwasawa, *J. Catal.* **2000**, *196*, 56–65.
- [12] A. Martino, S. A. Yamanaka, J. S. Kawola, D. A. Loy, *Chem. Mater.* **1997**, *9*, 423–429.
- [13] U.-A. Paulus, U. Endruschat, G.-J. Feldmeyer, T.-J. Schmidt, H. Bönemann, R.-J. Behm, *J. Catal.* **2000**, *195*, 383–393.
- [14] Y. Mizukoshi, R. Oshima, Y. Maeda, Y. Nagata, *Langmuir* **1999**, *15*, 2733–2737.
- [15] S. Papp, I. Dekany, *Colloid Polym. Sci.* **2001**, *279*, 449–458.
- [16] C. B. Hwang, Y.-S. Fu, Y.-L. Lu, S.-W. Jang, P.-T. Chou, C.-R. C. Wang, S.-J. Yu, *J. Catal.* **2000**, *195*, 336–341.
- [17] K.-T. Wu, Y.-D. Yao, C.-R. C. Wang, P. F. Chen, E.-T. Yeh, *J. Appl. Phys.* **1999**, *85*, 5959–5961.
- [18] R. P. Andres, J.-D. Bielefeld, J.-I. Henderson, D.-B. Janes, V.-R. Kolagunta, C.-P. Rubiak, W. J. Mahoney, R.-G. Osifchin, *Science* **1996**, *273*, 1690–1693.
- [19] N. Toshima, in: *Fine Particles Sciences and Technology. From Micro- to New Particles*, (Ed.: E. Pellizzetti), Kluwer, Dordrecht, **1996**, p 371.
- [20] S. V. Ley, C. Mitchell, D. Pears, C. Ramarao, J.-Q. Yu, W.-Z. Zhou, *Org. Lett.* **2003**, *5*, 4665–4668.
- [21] M. M. Demir, M. A. Gulgun, Y. Z. Menciloglu, B. Erman, S. S. Abramchuk, E. E. Makhaeva, A. R.

- Khokhlov, V. G. Matveeva, M. G. Sulman, *Macromolecules* **2004**, *37*, 1787–1792.
- [22] S. Kidambi, J. H. Dai, J. Lin, M. L. Bruening, *J. Am. Chem. Soc.* **2004**, *126*, 2658–2659.
- [23] B. P. S. Chauhan, J. S. Rathore, T. Bando, *J. Am. Chem. Soc.* **2004**, *126*, 8493–8500.
- [24] a) W. Solodenko, K. Mennecke, C. Vogt, S. Gruhl, A. Kirschning, *Synthesis* **2006**, 1873–1882; b) A. Drelinkiewicz, A. Waksmundzka, W. Makowski, J. W. Sobczak, A. Krol, A. Zieba, *Catal. Lett.* **2004**, *94*, 143–156.
- [25] Y.-B. Liu, C. Khemtong, J. Hu, *Chem. Commun.* **2004**, 398–399.
- [26] U. R. Pillai, E. Sahle-Demessie, *J. Mol. Catal. A* **2004**, *222*, 153–158.
- [27] M. Adlim, M. Abu Bakar, K. Y. Liew, J. Ismail, *J. Mol. Catal. A* **2004**, *212*, 141–149.
- [28] D. Tabuani, O. Monticelli, A. Chincarini, C. Bianchini, F. Vizza, S. Moneti, S. Russo, *Macromolecules* **2003**, *36*, 4294–4301.
- [29] M. Kralik, A. Biffis, *J. Mol. Catal. A: Chem.* **2001**, *177*, 113–138.
- [30] K. Sundmacher, H. Künne, U. Kunz, *Chem. Ing. Tech.* **1998**, *70*, 267–271.
- [31] W. Solodenko, H. Wen, S. Leue, F. Stuhlmann, G. Sourkouni-Argirusi, G. Jas, H. Schönfeld, U. Kunz, A. Kirschning, *Eur. J. Org. Chem.* **2004**, 3601–3610.
- [32] Reviews: a) G. Jas, A. Kirschning, *Chem. Eur. J.* **2003**, *9*, 5708–5723; b) A. Kirschning, W. Solodenko, K. Mennecke, *Chem. Eur. J.* **2006**, *12*, 5972–5990.
- [33] a) U. Kunz, A. Kirschning, H. Schönfeld, W. Solodenko, *J. Chromatogr. A* **2003**, *1006*, 241–249; b) U. Kunz, A. Kirschning, H.-L. Wen, W. Solodenko, R. Cecilia, C. O. Kappe, T. Turek, *Catal. Today* **2005**, *105*, 318–324; c) U. Kunz, H. Schönfeld, W. Solodenko, G. Jas, A. Kirschning, *Ind. Eng. Chem. Res.* **2005**, *44*, 8458–8467.
- [34] Applications: a) A. Kirschning, C. Altwicker, G. Dräger, J. Harders, N. Hoffmann, U. Hoffmann, H. Schönfeld, W. Solodenko, U. Kunz, *Angew. Chem.* **2001**, *113*, 4118–4120; *Angew. Chem. Int. Ed.* **2001**, *40*, 3995–3998; *Angew. Chem.* **2001**, *113*, 4118–4120; b) W. Solodenko, U. Kunz, G. Jas, A. Kirschning, *Bioorg. Med. Chem. Lett.* **2002**, *12*, 1833–1835.
- [35] a) M. Zecca, M. Kralik, M. Boaro, G. Palma, S. Lora, M. Zancato, B. Corain, *J. Mol. Catal. A* **1998**, *129*, 27–34; b) A. Biffis, B. Corain, Z. Cvengrosova, M. Hronec, K. Jerabek, M. Kralik, *Appl. Catal. A: Gen.* **1995**, *124*, 355–365; c) J. K. Cho, R. Najman, T. W. Dean, O. Ichihara, C. Muller, M. Bradley, *J. Am. Chem. Soc.* **2006**, *128*, 6276–6277.
- [36] Recent reviews on microwave chemistry: a) C. O. Kappe, *Angew. Chem.* **2004**, *116*, 6408–6443; *Angew. Chem. Int. Ed.* **2004**, *43*, 6250–6284; b) B. L. Hayes, *Al-drichimica Acta* **2004**, *37*, 66–77; c) B. A. Roberts, C. R. Strauss, *Acc. Chem. Res.* **2005**, *38*, 653–661; d) A. de La Hoz, A. Diaz-Ortiz, A. Moreno, *Chem. Soc. Rev.* **2005**, *34*, 164–178; e) L. Perreux, A. Loupy, *Tetrahedron* **2001**, *57*, 9199–9223.
- [37] CEM Voyager continuous flow single mode microwave system, see Experimental Section for details. For recent applications of this reactor, see: a) M. C. Bagley, R. L. Jenkins, M. C. Lubinu, C. Mason, R. Wood, *J. Org. Chem.* **2005**, *70*, 7003–7006; b) T. N. Glasnov, D. J. Vugts, M. M. Koningstein, B. Desai, W. M. F. Fabian, R. V. A. Orru, C. O. Kappe, *QSAR Comb. Sci.* **2006**, *25*, 509–518; c) J. S. Smith, F. J. Iglesias-Sigueenza, I. R. Baxendale, S. V. Ley, *Org. Biomol. Chem.* **2007**, *5*, 2758–2761.
- [38] a) I. R. Baxendale, C. M. Griffiths-Jones, S. V. Ley, G. K. Tranmer, *Chem. Eur. J.* **2006**, *12*, 4407–4416; b) G. Shore, S. Morin, M. G. Organ, *Angew. Chem.* **2006**, *118*, 2827–2832; *Angew. Chem. Int. Ed.* **2006**, *45*, 2761–2766, and references cited therein; c) P. Watts, S. J. Haswell, *Chem. Eng. Technol.* **2005**, *28*, 290–301.
- [39] a) J. R. Thomas, *Catal. Lett.* **1997**, *49*, 137–141; b) W. L. Perry, D. W. Cooke, J. D. Katz, A. K. Datye, *Catal. Lett.* **1997**, *47*, 1–4.
- [40] The selective heating of metallic nanoparticles by microwaves has received considerable attention lately, and applications have ranged from improving catalytic performance and enhancing nanoparticle growth, to various biomedical applications. For example, see: a) Review: M. Tsuji, M. Hashimoto, Y. Nishizawa, M. Kubokawa, T. Tsuji, *Chem. Eur. J.* **2005**, *11*, 440–452; b) J. A. Gerbec; D. Magana, A. Washington, G. F. Strouse, *J. Am. Chem. Soc.* **2005**, *127*, 15791–15800; c) J. C. Yu, X. Hu, Q. Li, L. Zhang, *Chem. Commun.* **2005**, 2704–2706; d) M. J. Kogan, N. G. Bastus, R. Amigo, D. Grillo-Bosch, E. Araya, A. Turiel, A. Labarta, E. Giralt, V. F. Puntes, *Nano Lett.* **2006**, *6*, 110–115; e) G. S. Vanier; *Synlett* **2007**, 131–135; f) B. C. Ranu, A. Saha, R. Jana, *Adv. Synth. Catal.* **2007**, *349*, 2690–2696.
- [41] B. Corain, K. Jerabek, P. Centomo, P. Canton, *Angew. Chem.* **2004**, *116*, 977–980; *Angew. Chem. Int. Ed.* **2004**, *43*, 959–962;.
- [42] This assumption was verified by using a mathematical model which also demonstrated that larger amounts of added cross-linker lead to considerable degree of cross-linking in the outer shell. U. Kunz, C. Altwicker, U. Limbeck, U. Hoffmann, *J. Mol. Catal. A, Chem.* **2001**, *177*, 21–32.
- [43] a) J. M. Kremsner, C. O. Kappe, *J. Org. Chem.* **2006**, *71*, 4651–4658; b) M. Hosseini, N. Stiasni, V. Barbieri, C. O. Kappe, *J. Org. Chem.* **2007**, *72*, 1417–1424.
- [44] A. C. Metaxas, R. J. Meredith, *Industrial Microwave Heating*, in: *IEE Power Engineering Series*, London, **1983**, Vol. 4.
- [45] J. Kurfürstova, M. Hajek, *Res. Chem. Intermed.* **2004**, *30*, 673–681.
- [46] The effect of hot spot effects as described here are highly dependent of the flow rate. Compared to 2 mLmin⁻¹ flow rate employed here, the hot spot should be totally suppressed at flow rates of 180 mLmin⁻¹: R. Cecilia, U. Kunz, T. Turek, *Chem. Eng. Proc.* **2007**, *47*, 870–881.
- [47] For a recent review, see: T. N. Glasnov, C. O. Kappe, *Macromol. Rapid Commun.* **2007**, *28*, 395–410.